

Nonlinear electric transport in graphene: Quantum quench dynamics and the Schwinger mechanism

Balázs Dóra^{1,2,*} and Roderich Moessner¹

¹Max-Planck-Institut für Physik komplexer Systeme, Nöthnitzer Str. 38, 01187 Dresden, Germany

²Department of Physics, Budapest University of Technology and Economics, Budafoki út 8, 1111 Budapest, Hungary

(Received 16 September 2009; revised manuscript received 18 March 2010; published 21 April 2010)

We present a unified view of electric transport in undoped graphene for finite electric field. The weak field results agree with the Kubo approach. For strong electric field, the current increases nonlinearly with the electric field as $E^{3/2}$. As the Dirac point is moved around in reciprocal space by the field, excited states are generated. This is analogous to the generation of defects in a finite-rate quench through a quantum-critical point, which we account for in the framework of the Kibble-Zurek mechanism. These results are also recast in terms of Schwinger's pair production and Landau-Zener tunneling. Other systems exhibiting a band structure with Dirac cones, in particular, cold atoms in optical lattices, should exhibit the same dynamics as well.

DOI: [10.1103/PhysRevB.81.165431](https://doi.org/10.1103/PhysRevB.81.165431)

PACS number(s): 81.05.U–, 64.60.Ht, 73.50.Fq

I. INTRODUCTION

The discovery of graphene, a single sheet of carbon atoms in a honeycomb lattice has triggered intense research recently^{1,2} not only because of its potential application in future electronic devices but also because of its fundamental physical properties: its quasiparticles are governed by the two-dimensional Dirac equation, and exhibit a variety of compelling (pseudo-) relativistic phenomena such as the unconventional quantum-Hall effect,³ a (possibly universal) minimal conductivity at vanishing carrier concentration,² Klein tunneling in p - n junctions^{4,5} and Zitterbewegung.⁶

Quantum transport and nonlinear responses driven by finite external fields represent a genuine nonequilibrium phenomenon, giving rise to, e.g., dielectric breakdown or Bloch oscillations.⁷ The quantum aspect of these effects is particularly pronounced in reduced dimensions. Therefore, two-dimensional Dirac electrons in finite electric fields, the subject of this work, provide a fascinating setting for studying these issues.

A simple picture of electronic transport in a finite electric field is drift transport as considered by Drude: carriers move ballistically ($p=eEt$) until they change their momentum by a scattering process, replacing the time t by the appropriate scattering time. The special features of Dirac electrons relevant for transport in finite field include: (i) their velocity is pinned to the “light cone” Fermi velocity, v_F , (ii) relativistic particles undergo pair production in strong electric fields, as predicted by Schwinger,⁸ and (iii) a uniform electric field modifies locally the geometry of the Fermi surface by moving the Dirac point around in momentum space [Eq. (4)]. Since massless Dirac electrons can be thought of as being critical, this can lead to the production of excited states, and should leave its fingerprints on transport in finite electric fields.

Landau-Zener dynamics, describing the (avoided) level crossing in a two-level system,⁹ represents the natural language to discuss Klein tunneling^{5,10} in graphene, and is ultimately connected to defect formation and quench dynamics through quantum-critical points (QCP),¹¹ described by the Kibble-Zurek mechanism^{12,13} of nonequilibrium phase tran-

sitions. Applying these ideas to graphene allows us to analyze the real-time dynamics of the current, after switching on the electric field, and to identify the various crossovers (summarized in Table I). Electric transport depends sensitively on the frequency, temperature, electric field, and scattering rate (ω , T , E , and Γ), and the obtained current depends strongly on how the $(\omega, T, E, \Gamma) \rightarrow 0$ limit is taken.^{14,15} Our results follow from taking the $\omega=T=0$ limits in a finite electric field.

II. 2+1 DIMENSIONAL DIRAC EQUATION

We focus on the 2+1 dimensional Dirac equation in a uniform, constant electric field in the x direction, switched on at $t=0$, through a time-dependent vector potential as $\mathbf{A}(t)=[A(t), 0, 0]$ with $A(t)=Et\Theta(t)$. The resulting time-dependent Dirac equation, describing low-energy excitations around one of the Dirac points, say the K point in the Brillouin zone for clean graphene, is written as

$$H = v_F \{ \sigma_x [p_x - eA(t)] + \sigma_y p_y \},$$

$$i\hbar \partial_t \Psi_p(t) = H \Psi_p(t), \quad (1)$$

where $v_F \approx 10^6$ m/s is the Fermi velocity of graphene and the Pauli matrices (σ) arise from the two sublattices² of the honeycomb lattice.

Due to this (pseudo-) spin structure, Eq. (1) represents a natural formulation for the study of Landau Zener dynamics as well. It is convenient first to perform a time-dependent unitary transformation¹⁶

TABLE I. Temporal evolution of the nonequilibrium current for clean graphene. Bloch oscillations show up for $t \geq t_{\text{Bloch}} \sim \hbar/eaE$ (Ref. 7) with a the honeycomb lattice constant.

| Classical | Kubo | Schwinger/Kibble-Zurek |
|-----------------|---|--|
| $t \ll \hbar/W$ | $\hbar/W \ll t \ll \sqrt{\hbar}/v_F eE$ | $\sqrt{\hbar}/v_F eE \ll t \ll t_{\text{Bloch}}$ |
| $j_x \sim Et$ | $j_x \sim E$ | $j_x \sim tE^{3/2}$ |

$$U^* H U = \sigma_z \epsilon_p(t). \quad (2)$$

This accomplishes two things. First, it brings us to the adiabatic basis in the Landau-Zener language,⁹ i.e., it tracks the evolution of the state for an infinitesimal electric field. Second, the form of Eq. (2) neatly distinguishes positive- and negative-energy solutions. However, the very same solutions could of course alternatively have been obtained in the original (diabatic basis) as well from Eq. (1).

The unitary matrix U accomplishing this transformation is

$$U = \frac{1}{\sqrt{2}} \begin{bmatrix} \exp(-i\varphi/2) & \exp(-i\varphi/2) \\ \exp(i\varphi/2) & -\exp(i\varphi/2) \end{bmatrix} \quad (3)$$

and the explicit form of the resulting energy spectrum $\epsilon_p(t)$ is given by

$$\epsilon_p(t) = v_F \sqrt{[p_x - eA(t)]^2 + p_y^2}, \quad (4)$$

where $\tan \varphi = p_y / [p_x - eA(t)]$.

Finally, the transformed time-dependent Dirac equation is given by

$$i\hbar \partial_t \Phi_p(t) = \left[\sigma_z \epsilon_p(t) - \sigma_x \frac{\hbar v_F^2 p_y e E}{2 \epsilon_p^2(t)} \right] \Phi_p(t), \quad (5)$$

$$\Psi_p(t) = U \Phi_p(t). \quad (6)$$

Note that the electric field appears in two guises in this equation, both altering the energy spectrum and inducing off-diagonal terms in the Hamiltonian, which is a consequence of the explicit time dependence of the unitary transformation ($-iU^* \partial_t U$).

This we supplement by an initial condition. We study a system initially in the ground state at half-filling, in which the lower (upper) Dirac cone is fully occupied (empty)

$$\Phi_p^T(t=0) = (0, 1). \quad (7)$$

Starting from this state, occupation of a state in the upper band ($\sigma_z = +1$) immediately signals that an excitation has been produced.

The current operator in the original basis is obtained through the equation of motion as $j_x = -ev_F \sigma_x$. Under the unitary transformation, it transforms into

$$j_x = -ev_F (\sigma_z \cos \varphi + \sigma_y \sin \varphi). \quad (8)$$

After switching on the electric field, the current of course acquires a finite expectation value. By denoting $\Phi_p^T(t) = [\alpha_p(t), \beta_p(t)]$, we obtain the following expression:

$$\begin{aligned} \langle j_x \rangle_p(t) = & -ev_F \{ \cos \varphi [|\alpha_p(t)|^2 - |\beta_p(t)|^2] \\ & + 2 \sin \varphi \operatorname{Re}[i\alpha_p(t)\beta_p^*(t)] \}. \end{aligned} \quad (9)$$

The first term is the current from particles residing on the upper or lower Dirac cone while the second one describes interference between them and is responsible for Zitterbewegung. Using QED terminology, the first and second terms are referred to as conduction and polarization current, respectively.¹⁷ In condensed matter, these are called intra-band and interband contributions, respectively.

This expression can be simplified considerably. First, note that charge conservation implies $|\alpha_p(t)|^2 - |\beta_p(t)|^2 = 2|\alpha_p(t)|^2 - 1$. The interference correction also simplifies since

$$\partial_t |\alpha_p(t)|^2 = 2 \operatorname{Re}[\alpha_p(t) \partial_t \alpha_p^*(t)]. \quad (10)$$

By using the transformed Hamiltonian, Eq. (5),

$$\hbar \partial_t \alpha_p^*(t) = i\epsilon_p(t) \alpha_p^*(t) - i \frac{\hbar v_F^2 p_y e E}{2 \epsilon_p^2(t)} \beta_p^*(t) \quad (11)$$

consequently

$$\partial_t |\alpha_p(t)|^2 = - \frac{v_F^2 p_y e E}{\epsilon_p^2(t)} \operatorname{Re}[i\alpha_p(t)\beta_p^*(t)] \quad (12)$$

since $\operatorname{Re}(i|\alpha_p(t)|^2) = 0$. As a result, the expectation value of the current only requires the knowledge of $n_p(t) = |\alpha_p(t)|^2$ as

$$\langle j_x \rangle_p(t) = -ev_F \left\{ \frac{v_F(p_x - eEt)}{\epsilon_p(t)} [2n_p(t) - 1] - 2 \frac{\epsilon_p(t)}{v_F e E} \partial_t n_p(t) \right\}. \quad (13)$$

The term independent of $n_p(t)$, namely, $ev_F^2(p_x - eEt)/\epsilon_p(t)$ vanishes at half-filling after momentum integration. In QED, this originates from charge conjugation symmetry,¹⁷ while in graphene, the same result is obtained by taking the full honeycomb lattice into account as in Ref. 18.

III. TIME EVOLUTION OF THE CURRENT

For $t < 0$, the upper/lower Dirac cone is empty/fully occupied. The quantity $n_p(t)$ measures the number of particles created by the electric field in the upper cone through Schwinger's pair production.⁸ In graphene, instead of particle-antiparticle pairs, electron-hole pairs are created. Therefore, the basic quantity to determine transport through graphene is $n_p(t)$.

We start by analyzing its behavior at weak electric fields perturbatively. In this case, we can set $E=0$ in Eq. (5) except in the numerator of the off-diagonal terms, and obtain

$$n_p(t) = \frac{(eE\hbar p_y)^2}{4v_F^2 |p|^6} \sin^2 \left(\frac{v_F |p| t}{\hbar} \right). \quad (14)$$

This approximation is valid for $|p| = \sqrt{p_x^2 + p_y^2} \gg eEt$, i.e., everywhere except for the close vicinity of the Dirac point.

Plugging this into Eq. (13), the first term is already second order in the electric field and does not contribute to linear response. The second (polarization) term gives, taking valley and spin degeneracies into account

$$\langle j_x \rangle = \frac{e^2 E}{2\pi\hbar} \int_0^\infty dp \frac{\sin(2v_F p t/\hbar)}{p} = \frac{e^2}{4\hbar} E. \quad (15)$$

The resulting dc conductivity is

$$\sigma = j/E = e^2 \pi / 2h \quad (16)$$

in accordance with Ref. 18.

This is the value of the ac conductivity at finite frequencies obtained from the Kubo formula^{2,19} and measured

also,²⁰ and since the model does not contain any additional energy scale, which would change the value of the ac response down to $\omega \rightarrow 0$, the same value for the dc conductivity sounds plausible. In this regime, all electrons propagate with the maximal velocity v_F , therefore the current is saturated, independent of time. Within our approach, the small field response is dominated by the Zitterbewegung.

The ultrashort time transient response ($tW \ll \hbar$ with W the bandwidth) can be thought of as being fully classical. Expanding Eq. (14), we obtain

$$\langle j_x \rangle_p(t) = e^2 v_F \frac{p_y^2}{|p|^3} Et, \quad (17)$$

which is independent of \hbar . The current rises linearly with time after the switch on as $\langle j_x \rangle(t) = 4e^2 EWt/\hbar^2$. The very same result follows from a classical Hamiltonian H_{cl} and its associated Hamilton equation

$$H_{cl} = v_F \sqrt{(p_x - eEt)^2 + p_y^2},$$

$$\partial_x = \frac{\partial H_{cl}}{\partial p_x} = \frac{v_F^2 (p_x - eEt)}{H_{cl}}, \quad (18)$$

which gives for the classical current, $j_{cl}(p, t) = -e \partial_x$, at short times as in Eq. (17). Dirac particles can therefore be accelerated as $\partial_t^2 x = eE/m_{xx}$ at short times. This can be recast to be in accord with Newton's equation if one defines an effective mass as $1/m_{xx} = \partial^2 H / \partial p_x^2 = v_F p_y^2 / |p|^3$, which originates from the finite curvature of a cut through the Dirac cone.

For the general time and electric field dependence, Eq. (1) can be solved analytically^{17,21} using the parabolic cylinder functions. However, these do not immediately yield a transparent analytical expression for the electric current for arbitrary electric field and time.

Nonetheless, to investigate the strong field, long time [specified in Eq. (23)] response of Dirac electrons, we can use the asymptotic expansion of these eigenfunctions,^{16,17} or equivalently we can rely on the WKB approach²² to determine $n_p(t)$ through the barrier penetration factor, similarly to narrow gap semiconductors.²³ As a result, we get

$$n_p(t) = \Theta(p_x) \Theta(eEt - p_x) \exp\left(-\frac{\pi v_F p_y^2}{\hbar e E}\right), \quad (19)$$

which is the celebrated pair production rate by Schwinger,^{8,17} a manifestation of Klein tunneling,⁵ and also the Landau-Zener transition probability⁹ between the initial and final levels. More precisely, the conditions for applicability are $(p_x, eEt - p_x) \gg |p_y|$.

This expression can be transparently understood invoking Landau-Zener physics. Two levels at $\pm p_x$, weakly coupled by p_y , level cross with time, ending up at $\pm(p_x - eEt)$. The transition is completed when both the initial and final levels are well separated, in which case the mixing between them is given by Eq. (19), as plotted in Fig. 1. Equation (19) describes the nonequilibrium momentum distribution in the upper Dirac cone while $1 - n_p(t)$ is that in the lower cone. Its momentum dependence is highly nonthermal, i.e., it is strongly asymmetric with respect to p_x while its decay in p_y is Gaussian.

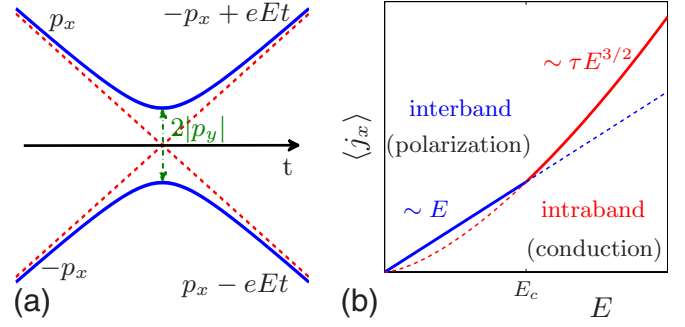


FIG. 1. (Color online) Left panel (a): visualization of the temporal evolution of the Landau-Zener dynamics. Right panel (b): schematic of the current-electric field characteristics for graphene. Interband transitions are overwhelmed by intraband ones with increasing electric field and the dominant contribution to the measured current changes in character from polarization to conduction.

Putting Eq. (19) into Eq. (13), one finds that the current is now dominated by the conduction (intraband part) as

$$\langle j_x \rangle(t) = \frac{2e^2 E}{\pi^2 \hbar} \sqrt{\frac{v_F e E t^2}{\hbar}}. \quad (20)$$

Crucially, the current now exhibits an increase which is linear in time, which at first glance appears to be quite analogous to what is observed for electrons in a conventional parabolic band.

However, the origin of the time dependence is completely different: it stems from the increasing number of pairs due to pair production à la Schwinger, each contributing with the same velocity v_F , as opposed to the continuously accelerated fixed number of normal electrons in strong fields. The $E^{3/2}$ dependence under distinct conditions has also shown up in Refs. 10, 14, and 24. The contribution of the polarization current reads in this range as

$$\langle j_x \rangle_{pol}(t) = \frac{2e^2}{\pi^3 \hbar} E, \quad (21)$$

which is overwhelmed by the intraband contribution.

As advertised above, the expectation value of the total number of particles-hole pairs created after the electric field is switched on, $N(t)$ can simply be obtained by considering $n_p(t)$

$$N(t) = \frac{2}{\hbar^2 \pi^2} \int d\mathbf{p} n_p(t) = \frac{2eE}{\pi^2 v_F \hbar} \sqrt{\frac{v_F e E t^2}{\hbar}}. \quad (22)$$

This leads to Eq. (20) via $\langle j_x \rangle(t) = e v_F N(t)$.

IV. RELATION TO QUANTUM QUENCH DYNAMICS

Equation (22) is related to the quench dynamics through a QCP,²⁵ relying on the Kibble-Zurek mechanism.^{12,13} This theory predicts the production of defects (excited states, vortices), when a system is driven through a QCP at a finite rate. In a continuous phase transition, the relaxation time of the system, which tells us how much time the system needs to adjust to new thermodynamic conditions, diverges at the

critical point due to critical slowing down. When the relaxation time becomes comparable to the ramping time close to the critical point, the system leaves the adiabatic regime and enters into a diabatic (impulse) one. In the latter region, its state is effectively frozen so that it cannot follow the time dependence of the instantaneous ground states—as a result, excitations are produced. The theory applies in many different fields of physics, such as the early universe cosmological evolution,¹² liquid ^{3,4}He (Refs. 13 and 26) or ultracold gases.²⁷

In the case of graphene, Eq. (1) can be diagonalized at every instant with eigenenergies in Eq. (4): the Dirac point moves continuously in momentum space with location $\mathbf{p} = (eEt, 0)$, which results in defect (excitation) production. The spectra from Eq. (4) can be considered as an ensemble of 1+1 dimensional, initially gapped systems (labeled by p_x) driven through a QCP. The initial energy gap is given by $v_F|p_x|$, the one-dimensional momentum is p_x , and the quench is applied as $v_F(p_x - eEt)$.

During the temporal evolution, the gap vanishes at the instant $t = p_x/eE$, and then reappears with increasing time. This effectively defines a QCP. It is characterized by the critical exponents $d = z = \nu = 1$.²⁵

The dynamics close to that QCP is necessarily nonadiabatic (impulse) due to the divergence of the relaxation time and the finite quench time $\sim 1/eE$.¹¹ The Kibble-Zurek mechanism^{12,13} predicts a scaling form for the defect formation as^{28,29} $E^{d\nu/(z\nu+1)} = E^{1/2}$ for a given 1+1 dimensional system.

However, defect production occurs only upon complete nonadiabatic passage through the QCP, i.e., for those initial states which have seen their gap close during the time evolution. At a given time t , this will be true for those values of the momentum satisfying $0 \ll p_x \ll eEt$. Obviously, this number of quenched “systems” scales linearly with both time and electric field, $\sim tE$. Combining these, the Kibble-Zurek mechanism thus also predicts the $tE^{3/2}$ scaling of the total defect density for Eq. (1), similarly to Eq. (22), linking the nonlinear transport in graphene to critical phenomena. (Quantum critical transport from a different perspective was already studied in Ref. 30.)

Therefore, the low field, perturbative response is dominated by interband contributions, and can be regarded as a manifestation of Zitterbewegung. With increasing field, a large number of electron-hole pairs are created, and intraband processes take over, producing nonlinear transport.

This crossover is determined by the dimensionless time scale, which can be obtained by comparing our system to the Landau Zener model as⁹

$$\tau_{cross} = \sqrt{\frac{v_F e E t^2}{\hbar}}. \quad (23)$$

For $\tau_{cross} \ll 1$, no level crossing occurs, and we can use perturbation theory to estimate the current, therefore we are in the Kubo regime. The Kibble-Zurek mechanism defines the freeze-out time^{11,13} by the instant \hat{t} when the system leaves the adiabatic regime and enters into the impulse one, namely, $\hat{t} = \hbar/(v_F e E \hat{t})$, and the Kibble-Zurek form of the defect

density requires complete transit through the QCP, $t \gg \hat{t} (\Leftrightarrow \tau_{cross} \gg 1)$.

In Landau Zener language, the level crossing is completed once $\tau_{cross} \gg 1$. The number of pairs created is nonperturbative in the electric field and we can use the probability of Landau-Zener tunneling to obtain an expression for the current.

V. TOWARD NONLINEAR TRANSPORT

So far we have discussed the real-time evolution of the current after the switch-on of the electric field, summarized in Table I. In ideal clean graphene, for long enough times, Bloch oscillation would set in due to the underlying honeycomb lattice structure. The next question which naturally arises is to what happens away from this highly idealized limit.

In the simplest approach, the time t will be replaced by an appropriate scattering time¹⁸ τ_{sc} . This could arise, in the spirit of Drude theory, from scattering due to phonons or impurities. Alternatively, in ballistic samples, ballistic flight time from the finite flake size, $\tau_b = L_x/v_F$ (Ref. 10) would assume that role. If the scattering is energy dependent, however, the nonlinear transport can take a different form, such as the one discussed in Ref. 14, which invoked the Schwinger mechanism for *interacting* bosons near a QCP.

The observation of nonlinear electric transport requires, from Eq. (23), an electric field as

$$E > E_c = \hbar/v_F e \tau^2, \quad (24)$$

where $\tau = \min(\tau_{sc}, \tau_b, \tau_\Delta)$ is the shortest of the additional restricting time scales (with τ_Δ defined below). Ballistic transport on the (sub-) μm scale implies $\tau \sim 0.1\text{--}1$ ps, giving $E_c \sim 10^3\text{--}10^5$ V/m.³¹

The exponents of the electric field of the linear (trivially 1) and nonlinear (3/2) regime do not differ significantly, and the measured current is expected to show a change of slope as a function of the electric field in the crossover region, and an extended electric field window would be required to reveal the noninteger exponent, as shown in Fig. 1. The linear (small E) region is independent of time through Eq. (15), naturally accounting for the scattering-independent minimal conductivity.

It is important to emphasize that in both regions, the current is related to $n_p(t)$. Thus, even the linear response regime witnesses pair production.

Recent transport measurements of undoped graphene devices have revealed superlinear current-voltage characteristics³² for strong voltages, with an exponent close to the predicted one (1.5), thus confirming our predictions and the realm of Schwinger’s pair production for graphene.

In the presence of a small mass gap, the above results need to be modified. The perturbative regime is characterized by exponentially activated behavior due to the gap and the current is exponentially suppressed at low temperatures ($T \ll \Delta$) as

$$j \sim E \exp(-\Delta/k_B T)$$

just as in normal semiconductors. On the other hand, for strong electric field, we can still use the analogy to Landau-Zener tunneling as

$$\langle j_x \rangle(t) = \frac{2e^2 E}{\pi^2 \hbar} \sqrt{\frac{v_F e E t^2}{\hbar}} \exp\left(-\frac{\pi \Delta^2}{\hbar v_F e E}\right). \quad (25)$$

Nonlinear transport sets in for $E > \pi \Delta^2 / \hbar v_F e$, which defines a new time scale for E_c as $\tau_\Delta = \hbar / \Delta \sqrt{\pi}$.

VI. OUTLOOK

In general, the nonlinear current for $d+1$ dimensional ($d=1, 2, 3$) Dirac electrons²¹ is

$$\langle j_x \rangle(t) \sim t E^{(d+1)/2} \exp\left(-\frac{\pi \Delta^2}{\hbar v_F e E}\right). \quad (26)$$

For $d=1$, a good realization would be carbon nanotubes (rolled-up graphene sheet), whose “nonlinear” response is still linear ($j \sim E$), only the nontrivial exponential factor with a possible gap reports about nonperturbative effects.³³ The $d=3$ case might be realized among the bulk electrons of Bi, possessing a band-gap ~ 0.015 eV.

These results are also relevant for other systems with possible Dirac fermions such as the organic conductor³⁴ α -(BEDT-TTF)₂I₃ with a tilted Dirac cone, or for topological insulators. Dirac fermions can be realized in cold atoms in an appropriate optical lattice (half-filled honeycomb, kagome, and triangular lattices), without any source of dissipation or scattering, a regime not naturally accessible for

materials-based condensed matter systems. The momentum distribution, Eq. (19), reveals the effect of the driving electric field before Bloch oscillations set in.⁷ The pairs created increase the energy of the system as $\sim t^2 E^{5/2}$, which, together with the highly nonthermal momentum distribution of Bloch states, can be measured after releasing the trap. This could be a first direct experimental observation of the Schwinger mechanism with microscopic resolution as well.

VII. CONCLUSIONS

In summary, we have studied the effect of finite electric field on graphene. While the weak field response is consistent with the Kubo approach, the strong field limit requires nonperturbative considerations. The Dirac point is moved around in the Brillouin zone by the field, which is related to quench dynamics through a quantum-critical point, and the current is obtained from the Kibble-Zurek mechanism. The crossover from linear to nonlinear transport is determined by the freeze-out time between the adiabatic and impulse regions. The nonlinear transport involves Schwinger’s pair production and Landau-Zener tunneling as well.

Note added. Recently we became aware of a related work.³⁵ Overlapping results are in agreement.

ACKNOWLEDGMENTS

We thank T. Cohen, D. McGady, and P. Thalmeier for stimulating discussions and comments, and support by the Hungarian Scientific Research Fund under Grant No. K72613 and by the Bolyai program of the Hungarian Academy of Sciences.

*dora@pks.mpg.de

¹K. S. Novoselov, A. K. Geim, S. V. Morozov, D. Jiang, Y. Zhang, S. V. Dubonos, I. V. Grigorieva, and A. A. Firsov, *Science* **306**, 666 (2004).

²A. H. Castro Neto, F. Guinea, N. M. R. Peres, K. S. Novoselov, and A. K. Geim, *Rev. Mod. Phys.* **81**, 109 (2009).

³K. S. Novoselov, A. K. Geim, S. V. Morozov, D. Jiang, M. I. Katsnelson, I. V. Grigorieva, S. V. Dubonos, and A. A. Firsov, *Nature (London)* **438**, 197 (2005).

⁴V. V. Cheianov and V. I. Fal’ko, *Phys. Rev. B* **74**, 041403(R) (2006).

⁵C. W. J. Beenakker, *Rev. Mod. Phys.* **80**, 1337 (2008).

⁶M. I. Katsnelson, *Eur. Phys. J. B* **51**, 157 (2006).

⁷M. Ben Dahan, E. Peik, J. Reichel, Y. Castin, and C. Salomon, *Phys. Rev. Lett.* **76**, 4508 (1996).

⁸J. Schwinger, *Phys. Rev.* **82**, 664 (1951).

⁹N. V. Vitanov and B. M. Garraway, *Phys. Rev. A* **53**, 4288 (1996).

¹⁰D. Allor, T. D. Cohen, and D. A. McGady, *Phys. Rev. D* **78**, 096009 (2008).

¹¹B. Damski, *Phys. Rev. Lett.* **95**, 035701 (2005).

¹²T. W. B. Kibble, *J. Phys. A* **9**, 1387 (1976).

¹³W. H. Zurek, *Nature (London)* **317**, 505 (1985).

¹⁴A. G. Green and S. L. Sondhi, *Phys. Rev. Lett.* **95**, 267001 (2005).

¹⁵A. W. W. Ludwig, M. P. A. Fisher, R. Shankar, and G. Grinstein, *Phys. Rev. B* **50**, 7526 (1994).

¹⁶T. D. Cohen and D. A. McGady, *Phys. Rev. D* **78**, 036008 (2008).

¹⁷N. Tanji, *Ann. Phys.* **324**, 1691 (2009).

¹⁸M. Lewkowicz and B. Rosenstein, *Phys. Rev. Lett.* **102**, 106802 (2009).

¹⁹K. Ziegler, *Phys. Rev. B* **75**, 233407 (2007).

²⁰R. R. Nair, P. Blake, A. N. Grigorenko, K. S. Novoselov, T. J. Booth, T. Stauber, N. M. R. Peres, and A. K. Geim, *Science* **320**, 1308 (2008).

²¹S. P. Gavrilov and D. M. Gitman, *Phys. Rev. D* **53**, 7162 (1996).

²²A. Casher, H. Neuberger, and S. Nussinov, *Phys. Rev. D* **20**, 179 (1979).

²³A. G. Aronov and G. E. Pikus, *Zh. Eksp. Teor. Fiz.* **51**, 281 (1966) [*Sov. Phys. JETP* **24**, 188 (1967)].

²⁴V. Ryzhii, M. Ryzhii, V. Mitin, and M. S. Shur, *Appl. Phys. Express* **2**, 034503 (2009).

²⁵J. Dziarmaga, *Phys. Rev. Lett.* **95**, 245701 (2005).

²⁶C. Bäuerle, Yu. M. Bunkov, S. N. Fisher, H. Godfrin, and G. R. Pickett, *Nature (London)* **382**, 332 (1996).

- ²⁷L. E. Sadler, J. M. Higbie, S. R. Leslie, M. Vengalattore, and D. M. Stamper-Kurn, *Nature (London)* **443**, 312 (2006).
- ²⁸A. Polkovnikov, *Phys. Rev. B* **72**, 161201(R) (2005).
- ²⁹C. De Grandi, V. Gritsev, and A. Polkovnikov, *Phys. Rev. B* **81**, 012303 (2010).
- ³⁰L. Fritz, J. Schmalian, M. Müller, and S. Sachdev, *Phys. Rev. B* **78**, 085416 (2008).
- ³¹J. Moser, A. Barreiro, and A. Bachtold, *Appl. Phys. Lett.* **91**, 163513 (2007).
- ³²N. Vandecasteele, A. Barreiro, M. Lazzeri, A. Bachtold, and F. Mauri, [arXiv:1003.2072](https://arxiv.org/abs/1003.2072) (unpublished).
- ³³A. V. Andreev, *Phys. Rev. Lett.* **99**, 247204 (2007).
- ³⁴S. Katayama, A. Kobayashi, and Y. Suzumura, *J. Phys. Soc. Jpn.* **75**, 054705 (2006).
- ³⁵B. Rosenstein, M. Lewkowicz, H. C. Kao, and Y. Korniyenko, *Phys. Rev. B* **81**, 041416(R) (2010).